Calcium-Binding Properties of Wild-Type and EF-Hand Mutants of S100B in the Presence and Absence of a Peptide Derived from the C-Terminal Negative Regulatory Domain of p53

Joseph Markowitz,[‡] Richard R. Rustandi,[‡] Kristen M. Varney,[‡] Paul T. Wilder,[‡] Ryan Udan,[‡] Su Ling Wu,[§] William DeW. Horrocks,[§] and David J. Weber*[,‡]

Department of Biochemistry and Molecular Biology, University of Maryland School of Medicine, 108 North Greene Street, Baltimore, Maryland 21201, and Department of Chemistry and Biochemistry and Molecular Biology, The Pennsylvania State University, University Park, Pennsylvania 16804

Received February 21, 2005; Revised Manuscript Received March 30, 2005

ABSTRACT: S100B is a dimeric Ca^{2+}-binding protein that undergoes a 90 ± 3° rotation of helix 3 in the typical EF-hand domain (EF2) upon the addition of calcium. The large reorientation of this helix is a prerequisite for the interaction between each subunit of S100B and target proteins such as the tumor suppressor protein, p53. In this study, Tb^{3+} was used as a probe to examine how binding of a 22-residue peptide derived from the C-terminal regulatory domain of p53 affects the rate of Ca^{2+} ion dissociation. In competition studies with Tb^{3+}, the dissociation rates of Ca^{2+} (k_{off}) from the EF2 domains of S100B in the absence and presence of the p53 peptide was determined to be 60 and 7 s^{-1}, respectively. These data are consistent with a previously reported result, which showed that that target peptide binding to S100B enhances its calcium-binding affinity [Rustandi et al. (1998) *Biochemistry 37*, 1951−1960]. The corresponding Ca^{2+} association rate constants for S100B, k_{on}, for the EF2 domains in the absence and presence of the p53 peptide are 1.1×10^6 and 3.5×10^5 M^{-1} s^{-1}, respectively. These two association rate constants are significantly below the diffusion control ($\sim 10^9$ M^{-1} s^{-1}) and likely involve both Ca^{2+} ion association and a Ca^{2+}-dependent structural rearrangement, which is slightly different when the target peptide is present. EF-hand calcium-binding mutants of S100B were engineered at the $-Z$ position (EF-hand 1, E31A; EF-hand 2, E72A; both EF-hands, E31A + E72A) and examined to further understand how specific residues contribute to calcium binding in S100B in the absence and presence of the p53 peptide.

S100B is a dimeric calcium-binding protein of the S100 protein family that is expressed in a large number of normal tissues including astrocytes and melanocytes (*1*−*6*). In general, S100 proteins respond to increasing Ca^{2+} levels inside the cell and regulate numerous biological processes including cell-cycle control, energy metabolism, and protein phosphorylation by binding to and regulating numerous protein targets in a calcium-dependent manner (*7*−*10*). One target protein is the tumor suppressor protein (p53),[1] which is ultimately down-regulated by S100B binding (*11*, *12*). In particular, S100B interacts with C-terminal negative regulatory and oligomerization domains of p53 and inhibits the cellular transcriptional activity of wild-type p53 by decreasing its protein levels inside the cell and proportionally diminishing its ultimate function as a tumor suppressor (*11*, *12*). In cases when p53 levels are too high, the tumor suppressor protein contributes to its own demise by up-regulating the transcription of S100B (*12*). This feedback loop for p53 is reminiscent of what is found for another negative regulator of p53, namely, mdm2 (*12*). However, the important distinction between mdm2 and S100B is that the interaction between S100B and p53 is calcium-dependent and provides an important link between calcium-mediated signal transduction and cell-cycle-dependent tumor suppression pathways. Therefore, understanding the "calcium switch" mechanism required for the p53−S100B interaction is important and likely can provide insights about inhibiting the S100B−p53 complex. In this regard, developing small molecule inhibitors of S100B is part of a therapeutic strategy to restore wild-type p53 function in cancers where S100B levels are elevated and wild-type p53 levels are diminished as is found in most malignant melanoma and astrocytomas (*11*−*13*).

There are several high-resolution 3D structures of S100B available that are useful for understanding the calcium-dependent interaction between S100B and its protein targets, such as p53 (*14*−*21*). In all of these structures, S100B is a symmetric dimer whose interface is composed of a large

* To whom correspondence should be addressed: Department of Biochemistry and Molecular Biology, University of Maryland School of Medicine, 108 N. Greene St., Baltimore, MD 21201, Telephone: (410) 706-4354. Fax: (410) 706-0458. E-mail: dweber@umaryland.edu.

‡ University of Maryland School of Medicine.

§ The Pennsylvania State University.

[1] Abbreviations: S100β, a subunit of dimeric S100B($\beta\beta$); S100B($\beta\beta$), dimeric S100B with noncovalent interaction at the dimer interface; p53, tumor suppressor protein; NMR, nuclear magnetic resonance; HSQC, heteronuclear single-quantum coherence; NOESY, nuclear Overhauser effect spectroscopy; HMQC, heteronuclear multiple-quantum coherence; PKC, protein kinase C; DTT, dithiothreitol; LB, Luria broth.

10.1021/bi050321t CCC: $30.25
Published on Web 04/21/2005

number of hydrophobic interactions consistent with its very high stability (K_D < 1 nM) (*22*). Furthermore, each S100B subunit has two EF-hand calcium-binding sites that are brought into close proximity by a small two-stranded antiparallel β sheet. The second EF-hand (EF2; residue 61−72) has the consensus sequence of "typical" EF-hand (*23*, *24*), and binds calcium more than 5-fold more tightly than the N-terminal EF-hand (EF1; residues 18−31). The pseudo-hand, EF1, has 14 rather than 12 residues, and several of the ligands to calcium are from backbone carbonyl oxygen atoms rather than side-chain carboxylate oxygen atoms as found in the more typical EF-hands (*23*−*26*). A central loop (loop 2; residues 42−50) connects the two calcium-binding domains and is often referred to as the "hinge region" of S100 proteins. This hinge region and the hydrophobic C-terminal loop are the least conserved regions of sequence among the S100 protein family members and are important for interactions with specific target proteins (*10*).

A comparison of 3D structures of apo- and Ca^{2+}-bound S100B illustrates a large rotation (∼90°) in the position of helix 3 upon Ca^{2+}-binding, exposing a hydrophobic cleft responsible for binding protein targets (*14*, *15*, *19*−*21*). This conformational change is required for the interaction with target proteins such as p53 (*27*). Upon S100B binding, protein kinase C (PKC)-dependent phosphorylation in the C-terminal negative regulatory domain of p53 is inhibited (*28*) and the p53 tetramer is dissociated (*29*, *30*). Furthermore, when a peptide derived from the negative regulatory domain of p53 binds to S100B, the affinity for Ca^{2+} in the typical EF-hand (EF2) of S100B increases by 3-fold (*27*). To further characterize Ca^{2+} binding and the resulting conformational change in S100B, we have measured rates of Ca^{2+} dissociation in the presence and absence of a peptide derived from residues 367−388 from the C terminus of p53 ($^{367-388}$p53 peptide). In these experiments, Ca^{2+} release is monitored in competition studies with Tb^{3+} using stopped-flow methods. The use of Tb^{3+} as a probe is ideal because of its unique luminescence properties at room temperature and because of its chemical similarity to the spectroscopically silent Ca^{2+} ion (*31*−*33*). In summary, we have now demonstrated that Ca^{2+} binding of the $^{367-388}$p53 peptide to S100B decreases the Ca^{2+} dissociation rate by about an order of magnitude. Furthermore, comparisons of wild-type and calcium-binding mutants of S100B (E31A, E72A, and E31A + E72A) provide additional information about how specific residues are involved in the "calcium switch" in the wild-type S100B protein.

MATERIALS AND METHODS

Materials. All chemical reagents were ACS-grade or higher unless otherwise indicated. Buffers were passed through Chelex-100 resin (Bio-Rad) to remove trace metals. Perdeuterated Tris, d_{11}-Tris (1 M solution in D_2O), D_2O, and $^{15}NH_4Cl$ were purchased from Cambridge Isotope Laboratories, Inc. $TbCl_3 \cdot 6H_2O$ was purchased from Sigma−Aldrich Chemical Co. (Sigma−Aldrich, St. Louis, MO). The Tb^{3+} and Ca^{2+} ion solutions were standardized by a titration method previously described (*34*).

S100B Protein and p53 Peptide Preparation. Recombinant S100B was prepared as previously described (*27*). Briefly, rat S100B was overexpressed in *Escherichia coli* strain HMS174(DE3) transformed with an expression plasmid containing a cDNA encoding S100B gene. Cells were grown in Luria broth (LB) containing 50 μg/mL ampicillin and induced with 0.2 mg/mL IPTG at OD_{600} = 0.8. S100B proteins were purified (>99%) under reducing condition using procedures similar to those described previously (*27*). For experiments with Tb^{3+}, the S100B was dialyzed extensively to remove any residual Tris buffer. The S100B subunit concentration was determined using the Bradford protein assay using S100B of a known concentration as the standard; the concentration of the standard S100B sample was determined via amino acid analysis (Analytical Biotechnology Services, Boston, MA).

A peptide, acetyl-SHLKSKKGQSTSRHKKLMFKTE-am, derived from human p53 (residues 367−388), was synthesized using solid-phase peptide synthesis (Biosynthesis, Inc., Lewisville, TX; Biopolymer Laboratory, University of Maryland School of Medicine, Baltimore, MD) with its N and C termini acetylated (acetyl-) and amidated (-am), respectively. The p53 peptide was stored as a lyophilized powder and dissolved in 1 mM Tris-d_{11}-HCl at pH 7.6 or 2 mM Hepes at pH 7.0 prior to use. The purity (>99%) of the p53 peptide was determined using HPLC and mass spectroscopy, and its concentration and composition were confirmed by amino acid analysis (Biosynthesis, Inc, TX; Analytical Biotechnology Services, Boston, MA).

Luminescence Spectroscopy. All luminescence spectra were collected on a SLM-Aminco series 2 luminescence spectrometer or a Varian Eclipse. The temperature of the cell was maintained at 22 °C using a circulating constant-temperature bath. Two approaches were used to measure calcium binding of wild-type and mutant forms of S100B. In the first approach, the quenching of tyrosine fluorescence (λ_{ex} = 275 nm; λ_{em} = 295−350 nm) was monitored as a function of adding terbium or calcium, as described previously (*27*). In the second approach, the emission of terbium (λ_{em} = 545 nm; λ_{ex} = 230) was monitored as a function of adding S100B. After titrations with terbium, calcium was added in competition experiments with terbium and the intensity of free terbium ions was restored. In these competition assays, the dissociation of calcium from S100B, $^{Ca}K_D$, was calculated using $^{Ca}K_D = K'/(1 + [Tb^{3+}]/^{Tb}K_D)$, where K' is from the best-fit curve of the titration data and $^{Tb}K_D$ is the dissociation constant for terbium from S100B. Titrations of Tb^{3+} into S100B (10−12 μM) in the absence or presence of p53 peptide (12−14 μM) were monitored by the increase of Tb^{3+} emission at 545 nm (λ_{ex} = 230 nm) or by energy transfer from tyrosine-17 of S100B (λ_{ex} = 275 nm) to Tb^{3+} (λ_{em} = 545 nm) to determine occupancy of the tight and weak sites as previously described (*32*). Once again, competition studies were performed with calcium to compete with the terbium. The p53 peptide was titrated into Tb^{3+}−S100B as measured by an increase in Tb^{3+} emission at 545 (λ_{ex} = 230 nm) to determine the K_D for the p53−Ca^{2+}−S100B complex. A λ < 500 nm cutoff filter in emission recordings was used to remove any interference from harmonic doubling. The ^{F385W}p53 mutant peptide (residues 367−388) in which Phe385 was mutated to a tryptophan was also used in binding experiments to wild-type and mutants of S100B (λ_{ex} = 295 nm; λ_{em} = 330−400 nm), as previously described for wild-type S100B (*27*). In these titrations, the p53 solution contained 20−25 μM ^{F385W}p53 peptide, 1 mM

$CaCl_2$, 50 mM Hepes at pH 7.0 and 22 °C, and the conditions were kept constant throughout the titration with wild-type and mutant S100B.

Nuclear Magnetic Resonance (NMR) Spectroscopy. Bruker Avance 600 MHz and Bruker Avance 800 MHz NMR spectrometers equipped with four frequency channels and triple resonance cryogenic probes were used to collect the NMR data. Data processing was performed on computers with the RedHat Linux operating system using the processing program NMRPipe (*35*), and data were viewed using NMRView (*36*). The backbone and side-chain chemical shifts of apo-S100B and Ca^{2+}-loaded S100B have been described previously (*15*, *18*, *23*). The assignments of mutant forms of ^{15}N-labeled S100B (apo and calcium loaded) could be made in most cases by inspection of a 2D ^{1}H-^{15}N fast heteronuclear single-quantum coherence (HSQC) (*37*), but three-dimensional nuclear Overhauser effect spectroscopy NOESY−HSQC data were collected nonetheless to confirm the assignments of all mutant forms of S100B (E31A, E71A, and E31A + E72A). For the mutant forms of calcium-loaded S100B (E31A and E72A S100B) bound to the p53 peptide, 3D ^{15}N,^{15}N-edited heteronuclear multiple-quantum coherence HMQC−NOESY−HSQC (*38*) data were also collected to confirm the resonance assignments. NMR sample conditions typically consisted of 75−900 μM S100B, 30 mM Tris-HCl, 0−25 mM $CaCl_2$, 0.3 mM NaN_3, 0.4 mM EDTA, 5 mM dithiothreitol (DTT), and 5% D_2O at pH 7.0 and 37 °C.

Stopped-Flow Measurements. Stopped-flow kinetic experiments were performed on a SF-2001 stopped-flow apparatus (KinTek Instruments Corporation, College Station, PA). Competition experiments with Tb^{3+} were used to measure the Ca^{2+} dissociation from S100B and were done by mixing the contents of syringe A containing S100B and various concentrations of $CaCl_2$ with the contents of syringe C containing $TbCl_3$. Both syringes contained 50 mM Hepes at pD 7.0 buffer in D_2O. Identical conditions were used for measurements of Ca^{2+} dissociation from the S100B−Ca^{2+}−p53 peptide complex except that the p53 peptide was also included in syringe A. The temperature in all experiments was maintained at 22 °C using a constant temperature water bath circulator. The reactions were initiated by mixing equal volume of both syringes and monitored by direct excitation of Tb^{3+} at 230 nm. Emission at $\lambda > 455$ nm ($\lambda_{max} = 545$ nm) was monitored and a $\lambda < 450$ cutoff filter was used.

The apparent dissociation rate constant of Ca^{2+}, k_{obs}, were obtained by recording 3−5 traces and taking an average of the data. The average values were fit to a single-exponential function, and the k_{off} of Ca^{2+} was obtained by fitting k_{obs} from the kinetic traces to the following equation:

$$k_{obs} = \frac{{}^{Ca}k_{off} + {}^{Tb}k_{off}\dfrac{{}^{Ca}k_{off}[Ca^{2+}]_t}{{}^{Tb}k_{off}[Tb^{3+}]_t}}{\dfrac{{}^{Ca}k_{off}[Ca^{2+}]_t}{{}^{Tb}k_{off}[Tb^{3+}]_t} + 1} \quad (1)$$

where $[Ca^{2+}]_t$ and $[Tb^{3+}]_t$ are total concentrations. The measured k_{obs} data were plotted as a function of $[Ca^{2+}]_t/[Tb^{3+}]_t$ and allow the determination of ${}^{Ca}k_{off}$ as previously described (*39*).

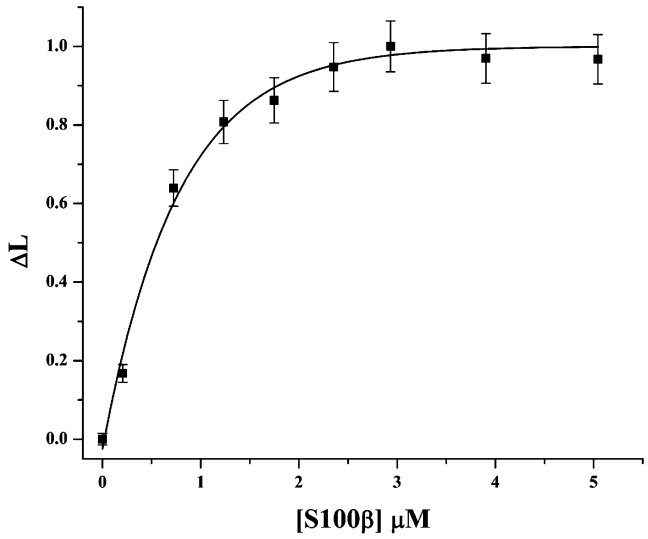

FIGURE 1: Representative titration of Tb^{3+} binding to the tight site of S100B (EF2) as monitored by changes in luminescence (ΔL) at 545 nm. The Tb^{3+} solution was excited at 230 nm, and the luminescence was measured at 545 nm with a 500 nm cutoff filter. Each subunit of S100B binds a single Tb^{3+} ion in the tight site ($^{EF2}K_D = 630 \pm 95$ nM); therefore, the concentrations listed for S100B are for a single subunit (S100β) of the symmetric dimer. The Tb^{3+} solution contains 1 μM $TbCl_3$ and 50 mM Hepes at pD 7.0 in D_2O and 22 °C.

RESULTS

Characterization of Tb^{3+} and Ca^{2+} Dissociation from the Wild-Type S100B−Metal and the S100B−Metal−p53 Complexes. In this study, terbium was used as a probe to monitor calcium binding of S100B in steady-state and kinetic luminescence measurements. Tb^{3+} can replace Ca^{2+} in S100B because of its similar effective ionic radii (0.98 versus 1.06 Å, respectively), and it maintains the biological activity of many EF-hand-containing protein systems (*31*, *33*, *40*). Upon binding Tb^{3+} to S100B, an increase of Tb^{3+} luminescence at 545 nm was monitored as a function of S100B subunit concentration, [S100β], using direct excitation ($\lambda_{ex} = 230$ nm; Figure 1) or tyrosine-sensitized Tb^{3+} emission ($\lambda_{ex} = 275$ nm) (*32*). The sequence of Tb^{3+} binding to EF2 was first confirmed using tyrosine-sensitized Tb^{3+} emission as described previously (*32*). After sufficient concentrations of Tb^{3+} are added to fully load the tight site, EF2 (EF2; EF1 < 10% occupied), further additions of Tb^{3+} induce tyrosine-sensitized emission at 545 nm consistent with it occupying the weak site (EF1). This occurs because Tb^{3+} is sensitized by a single tyrosine residue (Tyr-17) in S100B that is proximal to EF1 (residues 18−31) but distal to EF2 (*32*). The weak EF-hand, EF1, binds Tb^{3+} (EF1; $K_D > 10$ μM); however, the dissociation constant for this site could not be determined rigorously because the protein aggregates/precipitates at elevated Tb^{3+} concentrations as observed previously for S100B (*32*). For the other EF-hand (EF2), titration of Tb^{3+} into S100B using direct excitation ($\lambda_{ex} = 230$ nm) indicates that each S100B subunit binds a Tb^{3+} ion (EF2; residues 61−72) with a dissociation constant of 630 ± 95 nM (Figure 1). In competition studies with Ca^{2+}, only the high-affinity EF-hand, EF2, is fully loaded with Tb^{3+} and the fluorescence intensity of Tb^{3+} was restored as Ca^{2+} is titrated. Using this method, the dissociation constant for

Table 1: Dissociation of Ca^{2+} or p53 Peptide (^{F385W}p53) from Wild-Type and Mutants of S100B

calcium binding	EF1	EF2
wild-type S100B	>350 μM[a]	56 ± 9 μM[b]
E31A	>500 μM	>500 μM
E72A	480 ± 130 μM	>500 μM
E31A + E72A	>2 mM	>2 mM
wild-type S100B (+ p53)		20 ± 3 μM[c]
E31A		21 ± 7 μM[d]
E72A		18 ± 4 μM[d]
E31A + E72A		>300 μM
p53 peptide binding (^{F385W}p53)		
wild-type S100B	6.4 ± 1.1 μM[c]	
E31A	8.3 ± 3.1 μM	
E72A	7.3 ± 1.4 μM	
E31A + E72A	>75 μM	

[a] The value listed is from a previously published paper (*27*) and was confirmed in this study. [b] The value listed is from a previously published paper (*27*) and was confirmed in this study. The dissociation rate constant for wild-type S100B was determined as described in the text via stopped-flow methods and is k_{off} = 60 ± 22 s^{-1}. The off rate together with the K_D enables the calculation of a macroscopic on-rate value of k_{on} = 1.1 × 10^6 M^{-1} s^{-1} that includes calcium association plus a large conformational change. [c] The value listed is from a previously published paper (*27*) and was confirmed in this study. [d] The K_D value was determined using competition studies of Ca^{2+} with the respective Tb^{3+}-bound S100B mutant in the presence of the p53 peptide. These data together with the calcium off-rate values measured for the E31A and E72A mutants of 7.1 ± 3.7 and 6.8 ± 2.0 s^{-1}, respectively, are sufficient to calculate on-rate values of 3.4 ± 2.0 × 10^6 and 3.7 ± 1.3 × 10^6 M^{-1} s^{-1} for the mutants.

calcium binding to EF2 was found to be within the error limits of values reported previously ($^{Ca}K_D$ = 56 ± 9 μM; Table 1) using other methods (*27*). Only limiting values could be determined using such competition studies when estimating the dissociation of calcium from the weak site (EF1; K_D > 350 μM). Overall, it was determined that Tb^{3+} can be used as a probe to examine binding to EF2 and can be competed away using Ca^{2+} without any problems arising from precipitation.

Tb^{3+} ion binding to S100B was also measured when bound to a peptide derived from residues 367−388 at the C terminus of p53 ($^{367-388}$p53 peptide) (*18*, *27*, *41*). As found in the absence of the peptide, tyrosine-sensitized energy transfer measured for Tb^{3+} titrations done in the presence of $^{367-388}$p53 showed once again that the typical EF-hand (EF2) was loaded first followed by loading of the pseudo-EF-hand (EF1). Furthermore, the displacement of Tb^{3+} from EF2 by Ca^{2+} was performed to ensure that Tb^{3+} occupies the same sites as Ca^{2+} when the target peptide is bound. The dissociation constant of Ca^{2+} from the p53−Ca^{2+}−S100B complex measured from this competition experiment was within error of that determined previously (K_D = 20 ± 3 μM) using other methods (*42*). Last, the use of terbium as a probe in the Ca^{2+}−S100B−p53 interaction is reasonable because the p53 peptide binds to Tb^{3+}−S100B at a relatively high affinity as monitored in two separate titrations including a luminescence titration monitoring p53 binding to Tb^{3+}−S100B (K_D = 3.1 ± 0.3 μM; data not shown) and by stopped-flow measurements (Figure 2). In the latter experiment, it was possible to estimate the dissociation of the p53 peptide from Tb^{3+}-bound S100B (K_D = 2.9 ± 0.5 μM) by monitoring a reduction in the rate of Ca^{2+} dissociation from S100B as a function of the p53 peptide concentration (Figure 2). Therefore, Tb^{3+} is a good probe in competition studies

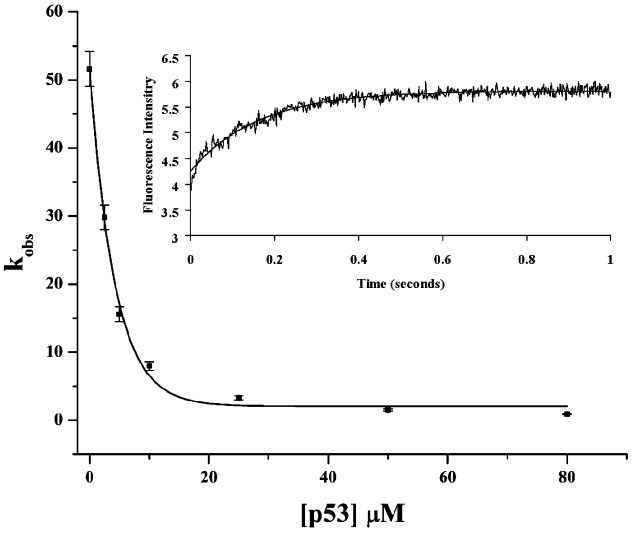

FIGURE 2: Decrease in the rate of calcium release (k_{obs}) from S100B as a function of the p53 peptide concentration (residues 367−388; $^{367-388}$p53). The k_{obs} values at each peptide concentration were calculated from kinetic traces of stopped-flow experiments where Tb^{3+} (syringe C) is mixed with calcium-loaded S100B at varying p53 peptide concentrations (syringe A) and the luminescence of Tb^{3+} is monitored (λ_{ex} = 230 nm; λ_{em} = 545 nm using a 450 nm cutoff filter) as a function of time. The trace shown in the inset was collected at 10 μM p53 peptide and fit to a single-exponential function. In all of the experiments, the concentration of the final mixed solution contained 10 μM S100β, 30 μM $TbCl_3$, 300 μM $CaCl_2$, 50 mM Hepes, and 0.05 mM DTT at pD 7.0 in D_2O and 22 °C.

for monitoring the kinetics of calcium dissociation from the tight EF-hand of S100B (EF2; Table 1).

The observed rate constant of Ca^{2+} release from S100B is determined by mixing various concentration of Ca^{2+} with Tb^{3+} and monitoring the increase of luminescence at λ > 450 nm (λ_{max} = 545 nm) with excitation at 230 nm as a function of time using stopped-flow techniques. Figure 3 (inset) shows the kinetic trace of Ca^{2+} dissociation from S100B at 300 μM concentration of Ca^{2+}. The data were fit to a single exponential, and the signal is attributed to the Ca^{2+} release from the tight site (typical EF-hand; EF2) of S100B. The observed first-order rate constant of Ca^{2+} release from the tight site of S100B is plotted against the ratio of $[Ca^{2+}]_t/[Tb^{3+}]_t$ and fit to a hyperbola to yield k_{off} of 60 ± 22 s^{-1} (Figure 3; eq 1). For comparison, the release of Ca^{2+} from S100B in the presence of p53 peptide was also measured and found to be 7.0 ± 3.2 s^{-1}. Thus, the presence of the p53 peptide was found to decrease the rate of dissociation of calcium by 8.5-fold for EF2. This result is in agreement with what was found previously, whereby the dissociation constant of calcium from S100B−Ca^{2+} (K_D = 56 ± 9 μM) was found to be tighter when the p53 peptide is present (K_D = 20 ± 3 μM; Table 1) (*27*). This decrease in the rate of Ca^{2+} dissociation is likely due to a conformational change that occurs in EF2 after the p53 peptide binds, which makes this EF-hand better suited to ligand calcium. The corresponding Ca^{2+} association rate constants for EF2 of S100B, k_{on}, in the absence and presence of the p53 peptide are 1.1 × 10^6 and 3.5 × 10^5 M^{-1} s^{-1}, respectively, indicating that Ca^{2+} association is 3-fold slower in the presence of the p53 peptide. Furthermore, these two association rate constants are significantly below diffusion control (~10^9 M^{-1} s^{-1}) and likely involve both Ca^{2+} ion association and a Ca^{2+}-

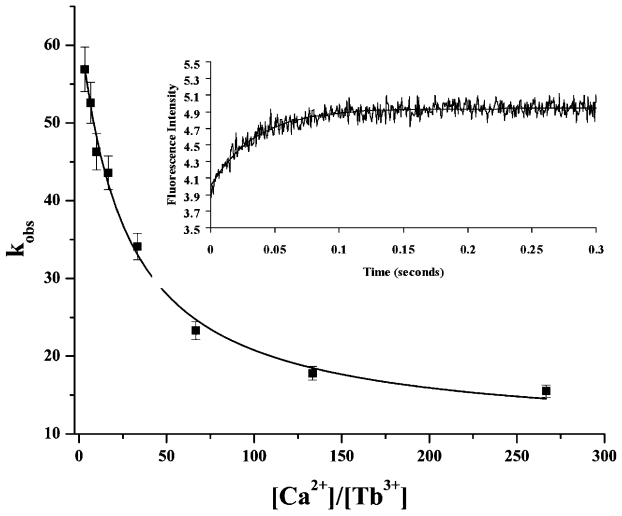

FIGURE 3: Decrease in k_{obs} as a function of $[Ca^{2+}]/[Tb^{3+}]$ used to determine the off rate of calcium from the typical EF-hand (EF2) of S100B ($^{Ca}k_{off}$). The k_{obs} values at each $[Ca^{2+}]/[Tb^{3+}]$ ratio were calculated from kinetic traces of stopped-flow experiments where Tb^{3+} (syringe C) is mixed with S100B at varying Ca^{2+} concentrations (syringe A) and the luminescence of Tb^{3+} is monitored (λ_{ex} = 230 nm; λ_{em} = 545 nm using a 450 nm cutoff filter) as a function of time. The trace shown in the inset was collected at 300 μM $CaCl_2$ concentration (i.e., 10:1 for $[Ca^{2+}]/[Tb^{3+}]$) and fit to a single-exponential function. In all of the experiments, the concentration of the final mixed solution contained 10 μM S100β, 30 μM $TbCl_3$, 50 mM Hepes, and 0.05 mM DTT at pD 7.0 in D_2O and 22 °C.

dependent structural rearrangement in S100B that is impeded somewhat by the presence of the p53 peptide.

Comparison of Wild-Type and EF-Hand Calcium-Binding Mutants (E31A, E72A, and E31A + E72A) of S100B via NMR Spectroscopy. Wild-type S100B binds calcium in the typical EF-hand (residues 61−72; $^{EF2}K_D = 56 \pm 9$ μM) more tightly than the pseudo-EF-hand (residues 18−31; $^{EF1}K_D >$ 350 μM), and a conformational change occurs upon binding EF2, which is necessary to bind target proteins such as p53 (*15*, *16*, *18*). One notable chemical-shift perturbation that occurs upon the addition of calcium to wild-type S100B is a 2.12 ppm downfield shift from 8.09 to 10.21 ppm (^{1}H; 1270 Hz at 600 MHz) for Gly66, which is in position 6 of the 12 consensus residues in EF2 (*43*). This and several other perturbations (>400 Hz; Figure 5B) are slow on the chemical-shift time scale and provide a limiting value for the rate of calcium ion dissociation (<400 s^{-1}). Furthermore, target peptide binding ($^{367-388}$p53) is found to enhance calcium binding by about 3-fold in the typical EF-hand ($^{EF2}K_D = 20 \pm 3$ μM) (*44*) despite the fact that no p53 peptide binding occurs in the absence of calcium even at high protein and peptide concentrations (>3 mM).

To examine the calcium-dependent S100B−target protein interaction more closely, calcium binding for S100B and various EF-hand mutants (E31A, E72A, and E31A + E72A) was examined by NMR. HSQC spectra were obtained for the E31A, E72A, and E31A + E72A mutants of S100B and compared to wild-type protein in the absence and presence of calcium and the $^{367-388}$p53 peptide. In the apo states, the chemical-shift values for the E31A, E72A, and E31A + E72A mutations were minimally different from those reported previously for wild-type S100B (*23*), and the perturbations that were observed are for the most part localized to the general area of the mutation (Figure 4), which is

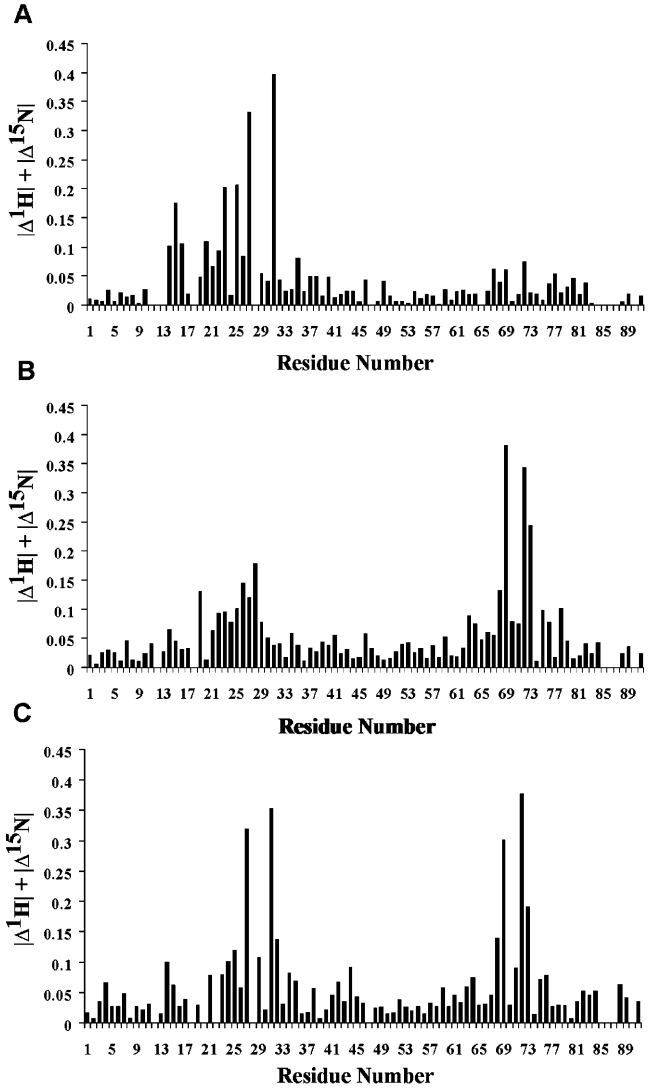

FIGURE 4: Comparisons of ^{1}H (600 MHz) and ^{15}N (61 MHz) chemical shifts of wild-type S100B to the (A) E31A, (B) E72A, and (C) E31A + E72A mutants of S100B in the absence of calcium (i.e., apo-S100B). Conditions included 275−900 μM wild-type or mutant S100B, 30 mM Tris, 5 mM DTT, 0.33 mM NaN_3, and 5% D_2O at pH 7.0 and 37 °C. Scaling on the *y* axis was achieved by normalizing the chemical-shift perturbations to the largest chemical-shift changes (^{1}H, ^{15}N) between apo- and Ca^{2+}-bound S100B.

indicative that no large structural rearrangement or problem with folding occurs as a result of the mutation. However, unlike what was observed previously in calcium ion titrations with wild-type S100B (Figure 5B) (*15*), the addition of calcium drastically broadens almost all of the ^{1}H-^{15}N correlations for both the E72A and E31A mutants of S100B and the spectra does not improve even at very high levels of calcium (>20 mM); this broadening effect is most likely due to intermediate exchange dynamics on the chemical-shift time scale as a result of weakened calcium binding for the E31A and E72A single mutants of S100B. Whereas, for wild-type S100B, several residues involved in binding calcium disappear and then reappear later in the titration consistent with slow exchange kinetics on the chemical-shift time scale (Figure 5B) (*15*).

For the double mutant (E31A + E72A), however, very few residues are perturbed in Ca^{2+} titrations and the glycine residue at position 6 of EF2 (G66) is not dramatically downfield-shifted (0.031 ppm; ~20 Hz) even at 20 mM

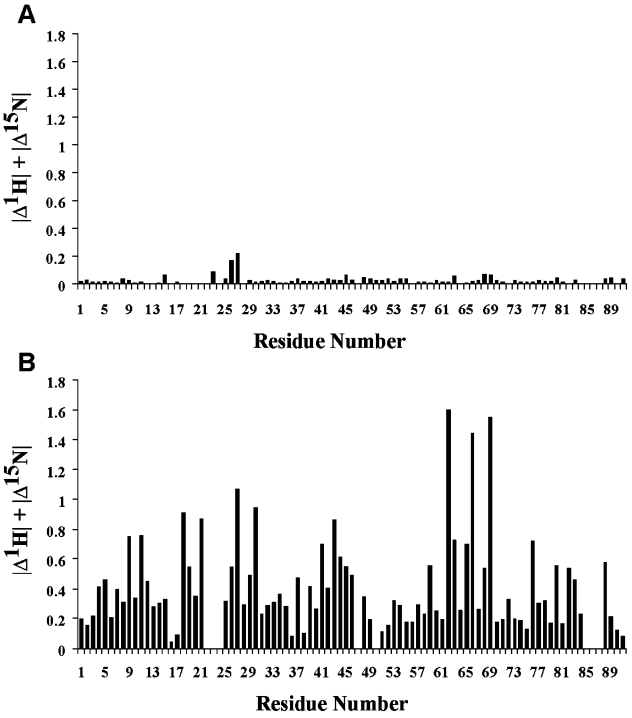

FIGURE 5: Chemical-shift perturbations (^{1}H, 600 MHz; ^{15}N, 61 MHz) observed upon the addition of calcium to the E31A + E72A double mutant (A) and to wild-type S100B (B). (A) For the double mutant, conditions included 900 μM E31A + E72A S100B, 30 mM Tris, 5 mM DTT, $^1/_3$ mM NaN_3, 5% D_2O, and ±20 mM $CaCl_2$ at pH 7.0 and 37 °C. (B) For comparison, the previously reported chemical-shift perturbations upon the addition of calcium to wild-type S100B are shown (*15*). Scaling on the *y* axis was achieved by normalizing the chemical-shift perturbations to the largest chemical-shift changes (^{1}H, ^{15}N) between apo- and Ca^{2+}-bound S100B.

calcium (Figure 5). These results are evidence that the E31A + E72A double mutant binds calcium very weakly if at all (>20 mM) and cannot properly change conformation as is necessary to bind target proteins such as p53 (Figure 5). The only calcium-dependent chemical-shift perturbations that were observed for the E31A + E72A double mutant (>0.15 ppm; >100 Hz) were for residues K26 and L27 in EF1, but these changes were very small and were observed only at very high levels of calcium (>5 mM). Interestingly, when the $^{367-388}$p53 peptide was added to Ca^{2+}−E31A-S100B, the HSQC spectrum was once again assignable, the downfield-shifted Gly66 residues appeared at 10.31 ppm (^{1}H), and relatively small chemical-shift differences were observed when comparing the ^{1}H and ^{15}N resonance assignments of the Ca^{2+}−E31A−p53 and the Ca^{2+}−WT-S100B−p53 complexes (Figure 6). Similar observations to those for E31A were observed for the E72A single mutant (Figure 6), indicating that the presence of the p53 peptide restores the ability of the E31A and the E72A single mutants to bind both calcium and target peptide.

Comparisons of Calcium and p53 Peptide Binding of Wild-Type and EF-Hand Mutants (E31A, E72A, and E31A + E72A) of S100B. To examine the calcium-dependent S100B−target protein interaction more closely, calcium binding to wild-type S100B and various EF-hand mutants (E31A, E72A, E31A + E72A) were examined via competition experiments with Tb^{3+} and by monitoring tyrosine fluorescence as a function of adding calcium (Table 1). For the E31A + E72A double mutant, no measurable calcium binding was observed

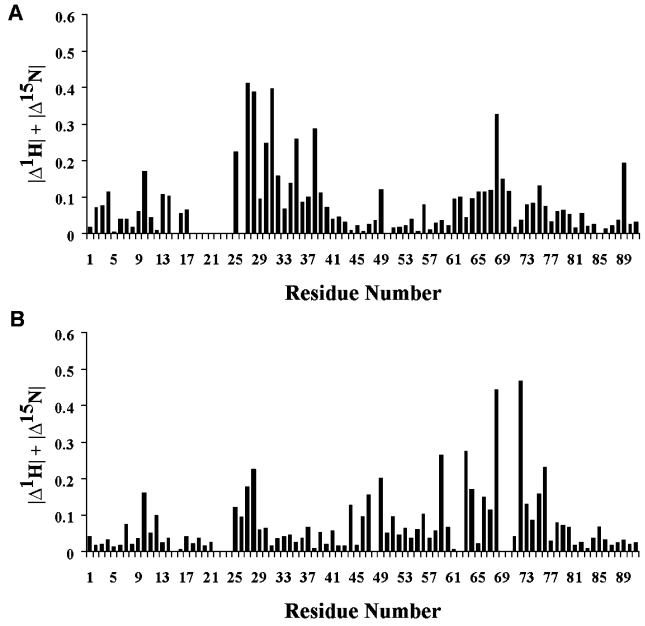

FIGURE 6: Comparisons of ^{1}H (600 MHz) and ^{15}N (61 MHz) chemical shifts of the wild-type p53−Ca^{2+}−S100B complex to the (A) p53−Ca^{2+}−E31A S100B and (B) p53−Ca^{2+}−E72A S100B complexes. Scaling on the *y* axis was achieved by normalizing the chemical-shift perturbations to the largest chemical-shift changes (^{1}H, ^{15}N) between apo- and Ca^{2+}-bound S100B. Conditions included 275−400 μM mutant S100B, 500−800 μM p53, 30 mM Tris, 5 mM DTT, $^1/_3$ mM NaN_3, 5% D_2O, and 10 mM $CaCl_2$ at pH 7.0 and 37 °C.

(K_D > 2 mM) consistent with the HSQC NMR titrations described above. Therefore, it was not surprising that target p53 peptide could not properly induce the calcium-dependent conformational change in the double mutant as determined by NMR HSQC titrations ($^{367-388}$p53, $^{p53}K_D$ > 300 μM). Similarly, binding of the peptide was not observed using fluorescence binding measurements (^{F385W}p53 peptide, K_D > 75 μM; Figure 7). Likewise, very weak, if any, calcium binding was observed to the E31A single mutant ($^{EF1}K_D$ > 500 μM; $^{EF2}K_D$ > 500 μM) despite the fact that the typical EF-hand domain (EF2) was intact. For the E72A single mutant, calcium binding could be measured, but it was consistent with only a single calcium ion binding to the first EF-hand of each S100B subunit ($^{EF1}K_D$ = 480 ± 130 μM). The fact that this residual calcium binding ($^{EF1}K_D$ = 480 ± 130 μM) was indeed due to the pseudo-EF-hand was confirmed by observations of tyrosine-sensitized Tb^{3+} luminescence from Tyr17 to Tb^{3+}, which occurs only when Tb^{3+} is bound to EF1 as is described in detail previously (*32*). Consistent with what was observed by NMR titrations, it was also found that binding of the p53 peptide (^{F385W}p53) to the E31A and E72A single-mutant S100B proteins is nearly identical to that found for the wild-type protein, despite their large decreases in calcium binding in the absence of the peptide (Figure 7).

As found for thermodynamic titrations (NMR and fluorescence; Table 1), restoration of p53 binding to E31A and E72A was also observed in stopped-flow experiments. Under conditions where p53 is bound (>85%), the rate constant of Ca^{2+} release from the Ca^{2+}−E31A-S100B−$^{367-388}$p53 and Ca^{2+}−E72A-S100B−$^{367-388}$p53 complexes was determined via competition experiments with Tb^{3+} using stopped-flow techniques. As for the wild-type protein (Figure 2), the data

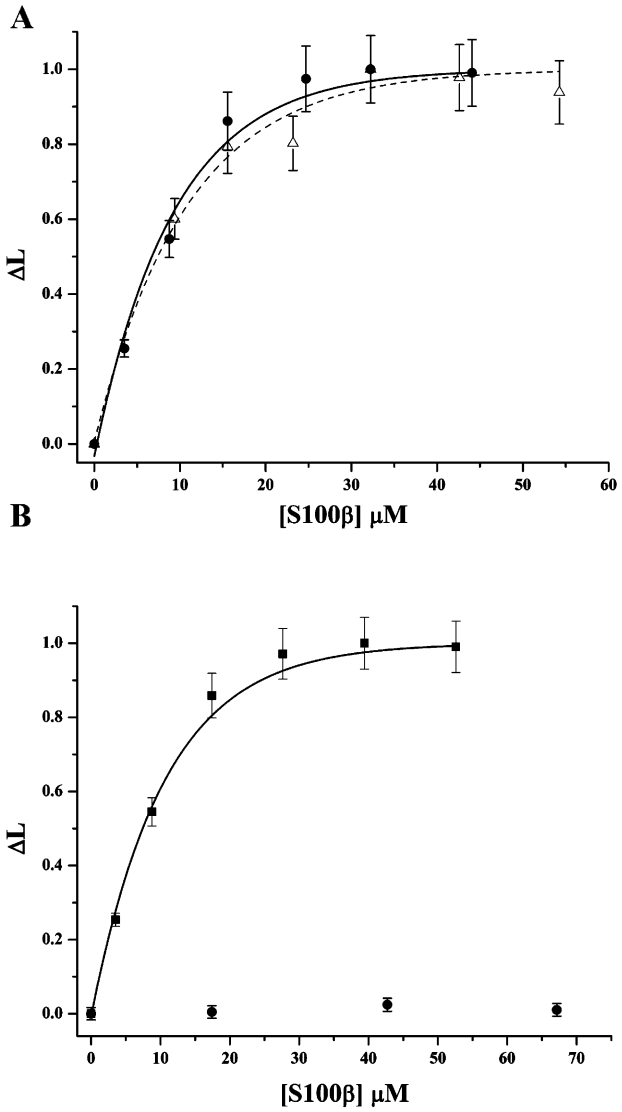

FIGURE 7: Representative titrations of the ^{F385W}p53 peptide binding to (A) the E31A single mutant of S100B (- - -), the E72A single mutant of S100B (—) and (B) wild-type S100B (—) and the E31A + E72A double mutant of S100B (●) as monitored by changes in fluorescence at 350 nm. The ^{F385W}p53 solution was excited at 295 nm, and the fluorescence was measured at 350 nm. The p53 solution contained 20−25 μM ^{F385W}p53 peptide, 1 mM $CaCl_2$, and 50 mM Hepes at pH 7.0 and 22 °C.

for the mutants were fit to a single exponential to yield rates of Ca^{2+} release from the tight site (typical EF-hand; EF2) of 6.8 ± 2.0 s^{-1} for the E31A mutant and 7.1 ± 3.7 s^{-1} for the E72A mutant, respectively (Table 1). These calcium off rates for the E31A and E72A mutants are indistinguishable from that observed for the analogous wild-type S100B−$^{367-388}$p53 complex ($^{Ca}k_{off}$ = 7.0 ± 3.2 s^{-1}; Figure 2). Likewise, the binding of Ca^{2+} to the E31A and E72A mutants was completely restored when p53 peptide is present as determined in steady-state competition studies with Tb^{3+} done in the presence of the p53 peptide (Table 1). These results indicate that the presence of a target peptide, such as p53 and ^{F385W}p53, completely restores the ability of these two single-mutant proteins to undergo the calcium-dependent conformational change as necessary to bind target peptide with high affinity (Table 1 and Figure 7). It is likely that a similar perturbation to the S100B structure occurs when $^{367-388}$p53 is present with wild-type holo-S100B and that this peptide-induced structural change is responsible for the increased calcium-binding affinity observed for wild-type S100B in the presence of p53 peptide.

DISCUSSION

S100B is a member of the S100 calcium-binding protein family that has a typical 12-residue EF-hand domain and an atypical 14-residue pseudo-EF-hand or "S100-hand" domain (*45*, *46*). Historically, the nomenclature for calcium coordination in calcium-binding proteins is that of an octahedral geometry with *X*, *Y*, *Z*, −*X*, −*Y*, and −*Z* coordination sites because it was originally thought the calcium ion had a octahedral coordination geometry; however, it is now recognized that calcium generally coordinates seven ligands in a pentagonal bipyramidal geometry (*24*). In a typical EF-hand such as EF2 of S100B (residues 61−72; EF2), the backbone carbonyl oxygen of the residue in the −*Y* position and side-chain oxygen atoms at the *Y* and *Z* positions together with an invariant glutamate, which provides two coordinating oxygen atoms at the −*Z* and −*Z*′, form an approximate coplanar pentagon. The side-chain oxygen atoms at positions *X* and −*X* are arranged at the two vertexes of the pentagonal plane with the −*X* position usually having an intervening H_2O molecule. Specifically, the Ca^{2+} ion bound to EF2 of S100B has six oxygen atoms coordinated from the protein including the carboxylate oxygen atoms of Asp61 (position 1), Asp63 (position 3), and Asp65 (position 5) at the *X*, *Y*, and *Z* sites, a backbone carbonyl oxygen from Glu67 (position 7) at the −*Y* site, and bidentate liganding from both carboxylate oxygen atoms of Glu72 (position 12) at the −*Z* and −*Z*′ sites (*15*, *20*, *32*). The bidentate ligand from the last position in the EF-hand domain is generally recognized to be critically important for initiating the conformational change observed in numerous EF-hand calcium-binding proteins (*24*). The final ligand is provided by a water molecule intervening between Asp69 (position 9) and the −*X* site of coordination such that the overall geometry of the calcium coordination sphere is pentagonal bipyramidal as found for most other EF-hand-containing proteins (*20*, *24*). Unlike the typical EF-hand (EF2), the pseudo-EF-hand of S100B (EF1; residues 18−31) has four ligands coordinated from backbone carbonyl oxygen atoms including Ser18, Glu21, Asp23, and Lys26 at the *X*, *Y*, *Z*, and −*Y* sites, respectively. Although, bidentate liganding from both carboxylate oxygen atoms of Glu31 at the −*Z* and −*Z*′ sites and a water ligand at the −*X* site of coordination are observed in the weak pseudo-EF-hand (EF1) as is the case for the typical EF-hand (EF2) of S100B (*20*).

In this study, we used Tb^{3+} as a probe to examine the calcium-binding properties of S100B in the presence and absence of a bound target peptide derived from the tumor suppressor protein, p53. Interestingly, it was discovered that the dissociation of Ca^{2+} from the typical EF-hand of S100B was nearly an order of magnitude slower in the S100B−Ca^{2+}−p53 peptide complex than from the S100B−Ca^{2+} complex, indicating that the calcium-coordination geometry is optimized when a target protein such as p53 is bound. Also revealing is the fact that the association rate constants for calcium both in the presence (k_{on} = 3.5 × 10^5 M^{-1} s^{-1}) and absence (k_{on} = 1.1 × 10^6 M^{-1} s^{-1}) of the peptide are both very slow relative to the diffusion control limit, consistent with the idea that the rates of Ca^{2+} association

include both stochastic interactions with the calcium-binding site plus a rearrangement of the EF-hand conformation. In S100B, positions *X*, *Y*, *Z*, and $-Z'$ need to be rearranged in the typical EF-hand to coordinate Ca^{2+}, whereas for proteins such as calmodulin, only the *Z* and $-Z$ positions need to be rearranged (*32*). Another difference between S100 proteins and other EF-hand family members is that for S100 proteins it is the entering helix that rotates upon binding calcium, whereas other EF-hand-containing proteins have the exiting helix rotate (*47*). Thus, it is important to examine S100B in the apo- and calcium-loaded state to understand the kinetics and conformational change(s) associated with calcium binding to this EF-hand subfamily. In S100B, as with many other EF-hand-containing proteins, the residue at position 12 of the EF-hand is critically important for this structural transition (*24*, *48*). Therefore, these residues were mutated in both the pseudo- and typical EF-hand domains of S100B (E31A, E72A, and E31A + E72A) and characterized using NMR, stopped-flow kinetics, and thermodynamic binding studies.

For the Glu72 → Ala mutation, calcium binding was abolished for the tight site (EF2), allowing for an accurate determination of binding to the weak site ($^{EF1}K_D = 480 \pm 130$ μM; Table 1). Furthermore, the amide proton and nitrogen resonances of Asp69 at position 9 in the typical EF-hand were significantly upfield-shifted in the mutant protein consistent with the lack of a hydrogen bond to the carboxylate oxygen atoms of Glu72. In addition, while some additional changes in the chemical shift were observed for residues in the pseudo-EF-hand with this mutation, the effects on Glu31 were minimal and the fact that this EF-hand does not change its conformation can likely explain why the pseudo-EF-hand retains its ability to bind calcium weakly. However, mutating position 12 (E31A) in the pseudo-EF-hand (EF1) was found to reduce calcium binding to the typical EF-hand by more than an order of magnitude. This result indicates that the EF-hand-binding domains are structurally linked in the apo- and/or calcium-bound state. Because the relative positioning of residues that ligand calcium in the typical EF-hand at positions *X*, *Y*, *Z*, and $-Z$ are significantly different upon binding calcium, it is likely that the mutation at position 31 in EF1 affects the positioning of one or more of these ligands in EF2 in the apo- and/or calcium-loaded state without affecting the global fold of the protein.

Another observation made in these studies is that binding of a peptide derived from the tumor suppressor protein, p53, restored the ability of the E31A and E72A mutant proteins to bind calcium. Restoration of calcium binding to each of the single mutants by the p53 peptide is consistent with there being an initial interaction between $Ca^{2+}-$S100B and p53 that precedes the large reorientation of helix 3. Binding of the p53 peptide to either of these singly loaded forms of S100B is sufficient to compensate for a mutation at the $-Z$ position introduced, and therefore, in the presence of the p53 peptide, the mutant S100B protein is now able to undergo the large conformational change, as judged by the large shift in the amide-proton HSQC correlation for Gly66. Furthermore, the dissociation of p53 from both the E31A and the E72A mutants are equivalent to that observed for the wild-type S100B (Figure 7).

A comparison of S100B to calbindin D9K, another well-characterized S100 protein, is a useful starting point for a kinetic model for calcium binding to S100B because it also contains typical and pseudo-EF-hand calcium-binding domains. For calbindin, calcium binds to both the pseudo- and typical EF-hand domains with relatively high affinity (pseudo-EF-hand, $^{EF1}K_D = 6.2 \pm 0.7$ nM; typical EF-hand, $^{EF2}K_D = 2.5 \pm 0.7$ nM) and is best characterized by a scheme described by Forsén and colleagues (*49*−*51*), in which calcium binds to either EF-hand domain, with two macroscopic equilibrium constants (K_1 and K_2), whereby P ⇔ P−Ca ⇔ P−$(Ca^{2+})_2$ and P is the protein, calbindin. However, a major difference between these two proteins is that a large degree reorientation of helix 3 occurs in the second EF-hand of S100B upon the addition of calcium that is not observed in calbindin (*15*, *51*, *52*). Therefore, the scheme for S100B needs to include this conformational change (A → B) such that A ⇔ A−Ca ⇔ B−Ca ⇔ B−$(Ca^{2+})_2$, where A and B represent S100B before and after the conformational change (Figure 8). The complete thermodynamic description of the calcium-dependent interaction of S100B with a target protein and a description of the relevant assumptions are presented fully in Appendix I in the Supporting Information. Because the binding of calcium to the pseudo-EF-hand is much weaker than that of the typical EF-hand, the pathway via K_{II}, L_I, and K_{XI} is predominant and is shown in bold (Figure 8; Appendix I in the Supporting Information). The importance of the 12 position for facilitating the conformational change, L_I, in the typical EF-hand (O →, Figure 8) is established here by mutagenesis studies in the second EF-hand (Glu72 → Ala) because mutating this residue severely inhibits the protein from fully loading calcium in this EF-hand. The addition of peptide to the E72A mutant is sufficient to restore the ability of S100B to undergo the conformational change by binding to a state where calcium is associated

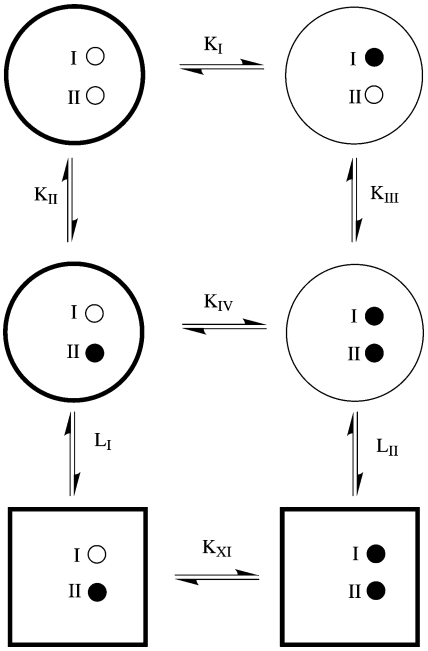

FIGURE 8: Schematic diagram illustrating the conformational changes and modes of calcium binding and dissociation from S100B. The predominant pathway for the calcium-dependent conformational change (via L_I) is shown in bold. The various equilibrium constants and the two possible conformational changes are defined in the text. See Appendix I in the Supporting Information for a full treatment of all of the possible thermodynamic equilibria.

with S100B prior to the conformational change. Although the populations of such sates are relatively low for wild-type S100B protein, they do exist in a full treatment of the thermodynamic equilibria (i.e., AM_IS, $AM_{II}S$, $AM_{I,II}S$; see Appendix I in the Supporting Information).

In summary, a large reorientation of helix 3 occurs in S100B upon binding calcium that is required for binding protein targets such as p53. In the presence of a protein target, the dissociation rate constant for calcium is decreased and the protein binds calcium with a higher affinity (in EF2). This conclusion is further supported by binding and kinetic data of S100B mutant proteins that have substitutions (Glu → Ala) at position 12 in the typical EF-hand (EF2; E72A) and pseudo-EF-hand (EF1; E31A), respectively. In the single- and double-mutant proteins, calcium binding is lost, but for both of the single-mutant proteins, calcium binding is completely restored when a target peptide derived from p53 is present. These results are consistent with p53 binding to a calcium-bound state of S100B that exists prior to the conformational change; it is p53 binding to this state that in turn facilitates the conformational change in the single-mutant proteins. Such a state also exists in the full thermodynamic treatment of the wild-type S100B; however, this state is not highly populated.

ACKNOWLEDGMENT

We are grateful to Dr. K. Johnson for use of his stopped-flow apparatus. This work was supported by grants from the National Institutes of Health (GM58888, to D.J.W.; F30-NS043916, to J.M.), the American Cancer Society (RPG0004001-CCG) to D.J.W., and the University of Maryland School of Medicine M.D./Ph.D. program to J.M.

SUPPORTING INFORMATION AVAILABLE

An appendix describing the complete thermodynamic cycle for the binding of calcium and target peptide to S100B. This material is available free of charge via the Internet at http://pubs.acs.org.

REFERENCES

1. Hauschild, A., Engel, G., Brenner, W., Glaser, R., Monig, H., Henze, E., and Christophers, E. (1999) S100B protein detection in serum is a significant prognostic factor in metastatic melanoma, *Oncology 56*, 338−344.
2. Hauschild, A., Michaelsen, J., Brenner, W., Rudolph, P., Glaser, R., Henze, E., and Christophers, E. (1999) Prognostic significance of serum S100B detection compared with routine blood parameters in advanced metastatic melanoma patients, *Melanoma Res. 9*, 155−161.
3. Mueller, A., Bachi, T., Hochli, M., Schafer, B. W., and Heizmann, C. W. (1999) Subcellular distribution of S100 proteins in tumor cells and their relocation in response to calcium activation, *Histochem. Cell Biol. 111*, 453−459.
4. Tan, M., Heizmann, C. W., Guan, K., Schafer, B. W., and Sun, Y. (1999) Transcriptional activation of the human S100A2 promoter by wild-type p53, *FEBS Lett. 445*, 265−268.
5. Suzushima, H., Asou, N., Hattori, T., and Takatsuki, K. (1994) Adult T-cell leukemia derived from S100β positive double-negative (CD4- CD8-) T cells, *Leuk. Lymphoma 13*, 257−262.
6. Takashi, M., Sakata, T., Nakano, Y., Yamada, Y., Miyake, K., and Kato, K. (1994) Elevated concentrations of the β-subunit of S100 protein in renal cell tumors in rats, *Urol. Res. 22*, 251−255.
7. Donato, R. (1999) Functional roles of S100 proteins, calcium-binding proteins of the EF-hand type, *Biochim. Biophys. Acta 1450*, 191−231.
8. Schafer, B. W., and Heizmann, C. W. (1996) The S100 family of EF-hand calcium-binding proteins: Functions and pathology, *Trends Biochem. Sci. 21*, 134−140.
9. Zimmer, D. B., Cornwall, E. H., Landar, A., and Song, W. (1995) The S100 protein family: History, function, and expression, *Brain Res. Bull. 37*, 417−429.
10. Weber, D. J., Rustandi, R. R., Carrier, F., and Zimmer, D. B. (2000) *Interaction of Dimeric S100B($\beta\beta$) with the Tumor Suppressor Protein: A Model for Ca-Dependent S100-Target Protein Interactions*, Kluwer Academic Publishers, Dordrecht, The Netherlands.
11. Lin, J., Blake, M., Tang, C., Zimmer, D., Rustandi, R. R., Weber, D. J., and Carrier, F. (2001) Inhibition of p53 transcriptional activity by the S100B calcium-binding protein, *J. Biol. Chem. 276*, 35037−35041.
12. Lin, J., Yang, Q., Yan, Z., Markowitz, J., Wilder, P. T., Carrier, F., and Weber, D. J. (2004) Inhibiting S100B restores p53 levels in primary malignant melanoma cancer cells, *J. Biol. Chem. 279*, 34071−34077.
13. Markowitz, J., Chen, I., Gitti, R., Baldisseri, D. M., Pan, Y., Udan, R., Carrier, F., MacKerell, A. D., and Weber, D. J. (2004) Identification and characterization of small molecule inhibitors of the calcium-dependent S100B−p53 tumor suppressor interaction, *J. Med. Chem. 47*, 5085−5093.
14. Drohat, A. C., Amburgey, J. C., Abildgaard, F., Starich, M. R., Baldisseri, D., and Weber, D. J. (1996) Solution structure of rat apo-S100B($\beta\beta$) as determined by NMR spectroscopy, *Biochemistry 35*, 11577−11588.
15. Drohat, A. C., Baldisseri, D. M., Rustandi, R. R., and Weber, D. J. (1998) Solution structure of calcium-bound rat S100B($\beta\beta$) as determined by NMR spectroscopy, *Biochemistry 37*, 2729−2740.
16. Drohat, A. C., Tjandra, N., Baldisseri, D. M., and Weber, D. J. (1999) The use of dipolar couplings for determining the solution structure of rat apo-S100B, *Protein Sci. 8*, 800−809.
17. Inman, K. G., Yang, R., Rustandi, R. R., Miller, K. E., Baldisseri, D. M., and Weber, D. J. (2002) Solution NMR structure of S100B bound to the high-affinity target peptide TRTK-12, *J. Mol. Biol. 324*, 1003−1014.
18. Rustandi, R. R., Baldisseri, D. M., and Weber, D. J. (2000) Structure of the negative regulatory domain of p53 bound to S100B($\beta\beta$), *Nat. Struct. Biol. 7*, 570−574.
19. Kilby, P. M., van Eldik, L. J., and Roberts, G. C. (1996) The solution structure of the bovine S100B protein dimer in the calcium-free state, *Structure 4*, 1041−1052.
20. Matsumura, H., Shiba, T., Inoue, T., Harada, S., and Kai, Y. (1998) A novel mode of target recognition suggested by the 2.0 Å structure of holo S100B from bovine brain, *Structure 6*, 233−241.
21. Smith, S. P., and Shaw, G. S. (1998) A novel calcium-sensitive switch revealed by the structure of human S100B in the calcium-bound form, *Structure 6*, 211−222.
22. Drohat, A. C., Nenortas, E., Beckett, D., and Weber, D. J. (1997) Oligomerization state of S100B at nanomolar concentration determined by large-zone analytical gel filtration chromatography, *Protein Sci. 6*, 1577−1582.
23. Amburgey, J. C., Abildgaard, F., Starich, M. R., Shah, S., Hilt, D. C., and Weber, D. J. (1995) ^{1}H, ^{13}C, and ^{15}N NMR assignments and solution secondary structure of rat Apo-S100β, *J. Biomol. NMR 6*, 171−179.
24. Strynadka, N. C., and James, M. N. (1989) Crystal structures of the helix−loop−helix calcium-binding proteins, *Annu. Rev. Biochem. 58*, 951−998.
25. Kretsinger, R. H. (1980) Structure and evolution of calcium-modulated proteins, *CRC Crit. Rev. Biochem. 8*, 119−174.
26. Baudier, J., Glasser, N., and Gerard, D. (1986) Ions binding to S100 proteins. I. Calcium- and zinc-binding properties of bovine brain S100$\alpha\alpha$, S100a($\alpha\beta$), and S100b($\beta\beta$) protein: Zn^{2+} regulates Ca^{2+} binding on S100b protein, *J. Biol. Chem. 261*, 8192−8203.
27. Rustandi, R. R., Drohat, A. C., Baldisseri, D. M., Wilder, P. T., and Weber, D. J. (1998) The Ca^{2+}-dependent interaction of S100B($\beta\beta$) with a peptide derived from p53, *Biochemistry 37*, 1951−1960.
28. Wilder, P. T., Rustandi, R. R., Drohat, A. C., and Weber, D. J. (1998) S100B($\beta\beta$) inhibits the protein kinase C-dependent phosphorylation of a peptide derived from p53 in a Ca-dependent manner, *Protein Sci. 7*, 794−798.
29. Delphin, C., Ronjat, M., Deloulme, J. C., Garin, G., Debussche, L., Higashimoto, Y., Sakaguchi, K., and Baudier, J. (1999)

Calcium-dependent interaction of S100B with the C-terminal domain of the tumor suppressor p53, *J. Biol. Chem. 274*, 10539−10544.
30. Baudier, J., Delphin, C., Grundwald, D., Khochbin, S., and Lawrence, J. J. (1992) Characterization of the tumor suppresor protein p53 as a protein kinase C substrate and a S100B-binding protein, *Proc. Natl. Acad. Sci. U.S.A. 89*, 11627−11631.
31. Bruno, J., Horrocks, W. D., Jr., and Zauhar, R. J. (1992) Europium(III) luminescence and tyrosine to terbium(III) energy-transfer studies of invertebrate (octopus) calmodulin, *Biochemistry 31*, 7016−7026.
32. Chaudhuri, D., Horrocks, W. D., Jr., Amburgey, J. C., and Weber, D. J. (1997) Characterization of lanthanide ion binding to the EF-hand protein S100 β by luminescence spectroscopy, *Biochemistry 36*, 9674−9680.
33. Horrocks, W. D., Jr., and Snyder, A. P. (1981) Measurement of distance between fluorescent amino acid residues and metal ion binding sites. Quantitation of energy transfer between tryptophan and terbium(III) or europium(III) in thermolysin, *Biochem. Biophys. Res. Commun. 100*, 111−117.
34. Fritz, J. S., Oliver, R. T., and Pietrzyk, D. (1958) *Anal. Chem. 30*, 1111−1114.
35. Delaglio, F., Grzesiek, S., Vuister, G. W., Zhu, G., Pfeifer, J., and Bax, A. (1995) NMRPipe: A multidimensional spectral processing system based on UNIX pipes, *J. Biomol. NMR 6*, 277−293.
36. Johnson, M. A., Rotondo, A., and Pinto, B. M. (2002) NMR studies of the antibody-bound conformation of a carbohydrate-mimetic peptide, *Biochemistry 41*, 2149−2157.
37. Mori, S., Abeygunawardana, C., Johnson, M. O., and van Zijl, P. C. (1995) Improved sensitivity of HSQC spectra of exchanging protons at short interscan delays using a new fast HSQC (FHSQC) detection scheme that avoids water saturation, *J. Magn. Reson. B 108*, 94−98.
38. Ikura, M., Bax, A., Clore, M., and Groneborn, A. M. (1990) Detection of nuclear Overhauser effects between degenerate amide proton resonances by heteronuclear three-dimensional nuclear magnetic resonance spectroscopy, *J. Am. Chem. Soc. 112*, 9020−9022.
39. Wu, S. L., Johnson, K. A., and Horrocks, W. D., Jr. (1997) Kinetics of formation of Ca^{2+} complexes of acyclic and macrocyclic poly(amino carboxylate) ligands: Bimolecular rate constants for the fully-deprotonated ligands reveal the effect of macrocyclic ligand constraints on the rate-determining conversions of rapidly formed intermediates to the final complexes, *Inorg. Chem. 36*, 1884−1889.
40. Horrocks, W. D., Jr., and Albin, M. (1984) *Prog. Inorg. Chem. 31*, 1−104.
41. Rustandi, R. R., Baldisseri, D. M., Drohat, A. C., and Weber, D. J. (1999) Structural changes in the C-terminus of Ca^{2+}-bound rat S100B ($\beta\beta$) upon binding to a peptide derived from the C-terminal regulatory domain of p53, *Protein Sci. 8*, 1743−1751.
42. Rustandi, R. R., Drohat, A. C., Baldisseri, D. M., Wilder, P. T., and Weber, D. J. (1998) The Ca^{2+}-dependent interaction of S100B with a peptide derived from p53, *Biochemistry 37*, 1951−1960.
43. Drohat, A. C., Baldisseri, D. M., Rustandi, R. R., and Weber, D. J. (1998) Solution structure of calcium-bound rat S100B as determined by nuclear magnetic resonance spectroscopy, *Biochemistry 37*, 2729−2740.
44. Tripos Associates, St. Louis, MO 63144.
45. Donato, R. (2001) S100: A multigenic family of calcium-modulated proteins of the EF-hand type with intracellular and extracellular functional roles, *Int. J. Biochem. Cell Biol. 33*, 637−668.
46. Heizmann, C. W., Fritz, G., and Schafer, B. W. (2002) S100 proteins: Structure, functions, and pathology, *Front. Biosci. 7*, 1356−1368.
47. Yap, K. L., Ames, J. B., Swindells, M. B., and Ikura, M. (1999) Diversity of conformational states and changes within the EF-hand protein superfamily, *Proteins 37*, 499−507.
48. Procyshyn, R. M., and Reid, R. E. (1994) A structure/activity study of calcium affinity and selectivity using a synthetic peptide model of the helix−loop−helix calcium-binding motif, *J. Biol. Chem. 269*, 1641−1647.
49. Forsen, S., Linse, S., Thulin, E., Lindegard, B., Martin, S. R., Bayley, P. M., Brodin, P., and Grundstrom, T. (1988) Kinetics of calcium binding to calbindin mutants, *Eur. J. Biochem. 177*, 47−52.
50. Linse, S., Brodin, P., Johansson, C., Thulin, E., Grundstrom, T., and Forsen, S. (1988) The role of protein surface charges in ion binding, *Nature 335*, 651−652.
51. Martin, S. R., Linse, S., Johansson, C., Bayley, P. M., and Forsen, S. (1990) Protein surface charges and Ca^{2+} binding to individual sites in calbindin D9k: Stopped-flow studies, *Biochemistry 29*, 4188−4193.
52. Johansson, C., Brodin, P., Grundstrom, T., Forsen, S., and Drakenberg, T. (1991) Mutation of the pseudo-EF-hand of calbindin D9k into a normal EF-hand. Biophysical studies, *Eur. J. Biochem. 202*, 1283−1290.

BI050321T